Journal of Biomedical Optics

BiomedicalOptics.SPIEDigitalLibrary.org

In vivo isolation of the effects of melanin from underlying hemodynamics across skin types using spatial frequency domain spectroscopy

Rolf B. Saager
Ata Sharif
Kristen M. Kelly
Anthony J. Durkin

SPIE.

Rolf B. Saager, Ata Sharif, Kristen M. Kelly, Anthony J. Durkin, "*In vivo* isolation of the effects of melanin from underlying hemodynamics across skin types using spatial frequency domain spectroscopy," *J. Biomed. Opt.* **21**(5), 057001 (2016), doi: 10.1117/1.JBO.21.5.057001.

In vivo isolation of the effects of melanin from underlying hemodynamics across skin types using spatial frequency domain spectroscopy

Rolf B. Saager,[a,*] Ata Sharif,[a] Kristen M. Kelly,[a,b] and Anthony J. Durkin[a]
[a]University of California, Irvine, Beckman Laser Institute and Medical Clinic, 1002 Health Sciences Road East, Irvine, California 92612, United States
[b]University of California, Irvine, Department of Dermatology, 118 Medical Surge 1, Irvine, California 92697, United States

Abstract. Skin is a highly structured tissue, raising concerns as to whether skin pigmentation due to epidermal melanin may confound accurate measurements of underlying hemodynamics. Using both venous and arterial cuff occlusions as a means of inducing differential hemodynamic perturbations, we present analyses of spectra limited to the visible or near-infrared regime, in addition to a layered model approach. The influence of melanin, spanning Fitzpatrick skin types I to V, on underlying estimations of hemodynamics in skin as interpreted by these spectral regions are assessed. The layered model provides minimal cross-talk between melanin and hemodynamics and enables removal of problematic correlations between measured tissue oxygenation estimates and skin phototype. [DOI: 10.1117/1.JBO.21.5.057001]

Keywords: oximetry; tissue optics; structured illumination; turbid media; optical properties; diffuse optical spectroscopy; spatial frequency domain; melanin.

Paper 150710RR received Oct. 23, 2015; accepted for publication Apr. 13, 2016; published online May 3, 2016.

1 Introduction

Techniques based on diffuse optical spectroscopic (DOS) principles can be applied to tissue to extract *in vivo* optical properties from tissue (i.e., absorption and reduced scattering coefficients).[1–3] These techniques may be deployed in a variety of measurement geometries ranging from probe-based point spectroscopy to wide-field imaging approaches and utilize a number of illumination/detection schema to exploit temporal and/or spatial responses from light interactions with tissue.[4–10]

Once these approaches characterize and isolate the effects of scattering, the remaining absorption properties are often interpreted as due to a linear superposition of chromophores in tissue, such as hemoglobin species (in either oxygenated or deoxygenated states), melanin, lipids, and water. The decomposition of tissue absorption spectra typically employs fitting methods (least-squares for example) resulting in estimates of chromophore concentrations or volume fractions relative to the total volume of tissue interrogated by the detected photons.

Spatial frequency domain techniques are, in general, based on DOS principles; these are noncontact techniques that entail the projection of structured illumination onto turbid media, such as skin. Camera-based imaging is used to detect the spatial frequency-dependent reflectance from the medium, at wavelengths of interest. Absorption and scattering can then be decoupled from reflectance measurements as each optical property will exhibit a differential response as a function of spatial frequency of illumination. This wide-field imaging approach has been applied for monitoring of port wine stain treatments and tissue transfer flap reperfusion and for assessments of burn wounds and nonmelanoma skin cancers.[11–21]

Spatial frequency domain spectroscopy (SFDS) (which we have formerly referred to as spatially modulated quantitative spectroscopy) is a spatial frequency domain method for which the detection scheme employs a fiber coupled spectrometer rather than a two-dimensional camera, thereby trading spatial resolution in favor of high spectral resolution (~1 nm) and spectral range (~400 to 1100 nm). As with many other diffuse optical measurement methods, SFDS has been validated through homogeneous optical phantoms of known optical properties, demonstrating that this technique is capable of quantifying the absorption and scattering properties of turbid media in both visible and near-infrared (NIR) wavelength regimes.[22]

Unlike the homogeneous phantoms used to validate these optical techniques, skin is a highly structured organ, consisting of several layers whose composition and function are differentiated. In the context of typical diffuse spectroscopic measurements, the detected spectral contributions from these stratified layers become a function of the thickness of each layer relative to the total volume of tissue interrogated by the optical technique. In the context of this work, we will refer to this as a partial volume effect.

Melanin is problematic in this case, as it has a relatively featureless absorption spectrum, typically described as a power-law spectral dependence,[23] yet can vary greatly in terms of its concentration and the partial volume it may occupy relative to the total volume interrogated by reflectance-based measurement techniques. These factors can present opportunities for cross-talk in spectral decomposition methods between determinations of melanin concentration and that of hemoglobin species. For example, errors in dermal oxygen saturation have been reported in regions of tissue underlying normal pigmented nevi as a consequence of incorrect accounting for epidermal melanin.[24] Similarly, in normal skin, the average local tissue oxygen saturation has been shown to trend inversely with the amount of

*Address all correspondence to: Rolf B. Saager, E-mail: rsaager@uci.edu

melanin in the skin as assessed across different skin colors (corresponding to pigmentation differences spanning Fitzpatrick types I to V), providing a clear indication that melanin can directly influence the interpretation of spectral signatures from blood.[25,26]

SFDS can also estimate the site-specific melanin layer thickness and the layer-specific concentration of melanin in skin based on its spectral response.[27] This approach does not assume any layer thickness, but rather leverages the differential penetration depth of visible and NIR wavelengths.[28] Fitting for chromophores in these two regions will produce concentrations of melanin and hemoglobin species, relative to the entire volume interrogated. By determining the absorption and reduced scattering coefficient at each wavelength, however, it is possible to also estimate the site-specific penetration depth, δ, from those spectral regions.[29] In the case of skin, visible light typically interrogates $\sim$100 μm whereas NIR wavelengths can penetrate millimeters through this spatial frequency approach. Assuming that melanin and hemoglobin are respectively confined within upper and lower layer structures, the differential determinations of melanin concentration by visible and NIR regimes can be used to describe the layer thickness in which melanin must reside in order to satisfy its respective concentration "detected per volume interrogated" in each regime. Whereas our previous study demonstrated that SFDS could characterize melanin with respect to multiphoton microscopy methods,[27] the question remains as to whether this method could then also produce optical properties that are truly faithful to the underlying physiology (e.g., hemodynamics in skin), once melanin is characterized.

In this study, we used both venous and arterial arm cuff occlusion paradigms to induce hemodynamic perturbations in the forearm. These occlusion paradigms have been used previously to illustrate and/or validate the sensitivity of optical methods in the context of monitoring hemodynamic changes in skin.[30] Whereas the occlusion paradigm will modulate tissue hemodynamics, our specific interest in this investigation is to assess the influence and potential sources of error that variations in skin pigmentation may impart in the determination of underlying hemoglobin. The accuracy and limitations of this approach are discussed within the context of quantitative, *in vivo* studies of skin hemodynamics.

We will interpret data collected by SFDS under these induced hemodynamic perturbations in three distinct ways: (1) homogenous fits (least-squares) in the visible regime (450 to 600 nm), (2) homogenous fits in the NIR regime (650 to 1000 nm), and (3) our own layered model approach (450 to 1000 nm).[28] From this single measurement platform, we are able to investigate the spectroscopic-based correlation between melanin and tissue hemodynamics independent from influences of differing measurement geometries or instrumentation sensitivity and performance.

2 Methods

2.1 *Clinical Study*

All subjects were treated in strict compliance with the declaration of Helsinki and the US Code of Federal Regulations for the protection of human subjects. The experiments were conducted with the full consent of each subject using a protocol approved by the internal review board (IRB) for human experiments in University of California, Irvine. Nine healthy subjects were enrolled under an IRB approved protocol (HS#2008-6307) (average age $= 35.6 \pm 8.3$ years, 3 female/6 male). Each subject was clinically assessed for skin type based on the Fitzpatrick scale[31] and ranged from skin type I to V. This skin-typing assessment method includes visual assessment of skin color, yet also considers hair color, eye color, and ethnic heritage (i.e., genetic disposition). Drs. Kelly and Sharif also clinically interviewed the subjects on (a) their tendency to burn and (b) the amount of sun exposure they receive (i.e., reaction to sun exposure and tanning habits) prior to assignment of a Fitzpatrick scale value. It is worth noting that this scale is not a direct descriptor of pigmentation, but rather a scale used to describe skin's response to sun exposure. Additionally, this assessment is qualitative and subjective. However, one predominant factor involved in this skin type assessment is the appearance of the amount of pigmentation, and for that reason alone, all subjects were classified by this scale. The spectroscopic measurements of melanin are not intended to be directly correlated to this scale, but to provide a general illustration of the range of pigmentation investigated in this study.

A blood pressure cuff occlusion protocol was used in this study as a means to externally perturb the hemodynamics of the forearm. In this study, we used an automated blood pressure cuff (E20, D. E. Hokanson, Inc.), which would inflate to 90 mmHg for venous occlusion and 200 mmHg for arterial occlusion. While venous pressure can be lower than 90 mmHg, we chose to work at this pressure in order to apply a consistent experimental protocol for all subjects and assure venous occlusions in all healthy subjects enrolled in this study. The imaging head of our instrument was placed over the volar forearm to monitor the distal effects of the cuff occlusion to the spectroscopic optical properties of the tissue. For each type of occlusion, the total acquisition sequence lasted 9 min, where each phase of the occlusion (i.e., baseline, occlusion, and release) lasted 3 min.

2.2 *Spatial Frequency Domain Spectroscopy Instrument*

The specific instrument used in this study (Fig. 1), an illumination source, a 100-W quartz-tungsten-halogen (QTH) light

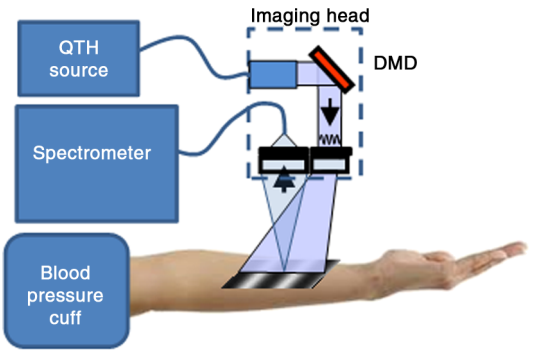

Fig. 1 System diagram and experimental setup: broadband illumination is delivered to the imaging head from a 100-W QTH lamp via a liquid light guide. The digital DMD then encodes the light into sinusoidal intensity patterns which are projected onto the surface of the volar forearm. Diffusely reflected light is delivered to the spectrometer via an optical fiber. An automated blood pressure cuff provides modulation of distal hemodynamics through either venous or arterial occlusions.

source (Moritex, MHF-D100LR) that was coupled to a digital micromirror device (DMD) (Texas Instruments, Inc. DLP) with a pattern projection area of 22×17 mm. From this projection configuration, tissue was illuminated with a sequence of sinusoidal intensity patterns that can span across a range of spatial frequencies up to 0.5 mm^{-1}. Remitted light from a 1-mm-diameter spot from tissue, centrally located in the illumination pattern projection area was collected by a fiber (NA 0.39, 1 mm core, Thorlabs, Inc.). Collected light was delivered to an Oriel spectrometer (Oriel 77480). The spectral response from tissue was recorded as a function of the spatial frequency at three evenly spaced phases (0 deg, 120 deg, and 240 deg) as we have previously described.[22]

Four evenly spaced spatial frequencies were employed, ranging from 0 to 0.3 mm^{-1}. A total of 12 spectral measurements were taken for a given data acquisition time point (four spatial frequencies, acquired at three evenly spaced phases per frequency). An autoexposure routine was performed prior to every occlusion time course series to ensure that the data collected uses the full dynamic range of the 16-bit detector. Additionally, three replicate accumulations were acquired and averaged at each projected pattern to help minimize noise. In its current configuration, this resulted in total acquisition times ranging from 10 to 30 s, depending on the amount of pigmentation present.

2.3 *Spatial Frequency Domain Spectroscopy Data Processing*

A three-phase demodulation scheme was employed at each spatial frequency to isolate the spatial frequency-dependent response from tissue from that of ambient light (e.g., ambient light, stray light from the instrument). Described in greater detail previously,[8] the demodulated raw reflectance signals at each spatial frequency were calibrated against a diffuse tissue simulating phantom of known optical properties to produce diffuse reflectance spectra as a function of spatial frequency. The calibration phantom is based in a polydimethylsiloxane medium with India ink as the absorbing agent and titanium oxide at the scattering agent, where absorption (μ_a) and reduced scattering (μ_s') coefficients are 0.02 and 1 mm^{-1} at 650 nm, respectively.[32] The response to spatial frequency was independently modeled at every wavelength to uniquely describe the absorption and reduced scattering coefficient at each wavelength. As this quantitative spectroscopic method spans both the visible and NIR domains, Monte Carlo methods were employed to comprehensively describe and solve for light transport in both diffusive (NIR) and nondiffusive regimes (visible). This approach has been independently validated for the determination of optical properties in homogeneous media.[22]

From this measurement platform, we have developed a layered model method to interpret these quantitative optical properties as a depth-segmented, two-layer system.[28] We have tested this model-based, depth-segmented approach in layered tissue simulating phantoms,[33] *in vivo* benign pigmented lesions, correlating the mean depths of pigmentation *in vivo* to high-frequency ultrasound,[34] as well as correlating melanin concentration and depth distribution in normal skin with multiphoton microscopy.[27] These previous studies have shown that this layered model approach can determine not only absolute depth-segmented concentrations of chromophores to within $\sim \pm 15\%$ but also the layer thickness that differentiates where these chromophores reside to within $\sim \pm 15$ μm. For this study, we used the spectral regions of 450 to 600 nm and 650 to 950 nm to represent the visible and NIR spectral regions in the aforementioned method. The outputs of this method are the top layer (optical) thickness (as determined by the absorption signature of melanin, relative to the mean photon pathlength traveled through the tissue) and the chromophore concentrations specific to the respective layers. The results of determining melanin concentration and top layer thickness are discussed in a previous study.[27] In the context of this investigation, however, we are interested in evaluating whether accounting for "layer-specific melanin concentration" and "melanin layer (mean distribution) thickness" would significantly impact the spectroscopic interpretation of underlying hemodynamics.

As the current SFDS instrument measured spatial frequency-dependent reflectance from 450 to 1000 nm, we evaluated the performance of multiple, standard spectral decomposition methods in the context of the same measurement geometry (avoiding inconsistencies derived from varied instrument configurations/calibrations and or other potential sources of variances). Once the SFDS data were processed and bulk absorption (μ_a) and reduced scattering (μ_s') coefficients are derived, we evaluated the performance of isolating and quantifying of hemodynamic trends from that of melanin when using (1) NIR spectra (650 to 1000 nm), (2) visible spectra (450 to 600 nm), or (3) our custom layer model method, using spectral information spanning both regimes (450 to 1000 nm).

2.4 *Analysis of Clinical Data*

For this investigation, we have chosen to present our results in two ways: (1) to demonstrate the isolation of detected melanin concentration from externally induced hemodynamic changes and (2) to illustrate the impact of this isolation of melanin in terms of physiologically relevant parameters related to the quantification of underlying hemoglobin. Whereas there are many ways to formulate metrics that would potentially address the performance and efficacy of this model-based approach in the context of tissue physiology, we have selected two specific metrics that would provide, in our estimation, the most unbiased, yet easily interpretable measures to evaluate the initial objectives of this investigation.

Isolation of detected melanin concentration from hemodynamics: Though the magnitude and temporal response of induced hemodynamics in these occlusion studies will vary from subject to subject, it is clearly understood that melanin concentration is physiologically invariant from these induced hemodynamic changes. Therefore, any changes detected in the determined concentration of melanin during these experiments are an indication of "cross-talk" between depth-specific chromophores present in skin (i.e., melanin versus hemoglobin concentration). We define Δmelanin as a metric to characterize the average change in melanin concentration estimation during the respective occlusions, relative to its baseline value

$$\Delta\text{melanin} = \text{abs}\left[\frac{\langle \text{mel}_{\text{conc}}(t)\rangle_{\text{occlusion}} - \langle \text{mel}_{\text{conc}}(t)\rangle_{\text{baseline}}}{\langle \text{mel}_{\text{conc}}(t)\rangle_{\text{baseline}}}\right].$$

Here $\langle \text{mel}\rangle_{\text{occlusion}}$ represents the average detected melanin concentration over the time period that the blood pressure cuff was inflated and $\langle \text{mel}\rangle_{\text{baseline}}$ represents the average melanin concentration prior to cuff inflation. This value will be specific to the spectral region and/or method used to determine melanin

concentration (i.e., visible, NIR, or layered model), and also specific to the type of occlusion performed (i.e., venous or arterial occlusion). This is a relative measure, specific toward either spectral region and/or spectral decomposition method's ability to minimize error/variance in the determination of melanin in the presence of hemodynamics.

Tissue oxygenation: Whereas the Δmelanin metric provides a measure of the relative cross-talk during the measurement, it does not describe any pre-existing cross-talk between chromophores at every measurement time point, independently. StO_2 is an optically derived measure of oxygen present in tissue based on the relative amounts of oxygenated and deoxygenated hemoglobin detected in the tissue microvasculature based on their distinct spectral features in both visible and NIR red regimes.[35] The use of this metric in the context of this investigation is not to validate one approach over another, but to examine the dependence of StO_2 as function of skin type and any general bias as a function of partial volume/depth of interrogation from specific wavelength regions

$$\langle StO_2\rangle_{\text{baseline}} = \frac{\langle HbO_2(t)\rangle_{\text{baseline}}}{\langle HbO_2(t) + Hb(t)\rangle_{\text{baseline}}} \times 100.$$

Here, $HbO_2(t)$ and $Hb(t)$ represent the temporally detected concentrations of oxy- and deoxyhemoglobin during the baseline period, as a determined by the spectral fits in visible, NIR and employing the layered model approach.

3 Results

Figures 2(a) and 2(c) present the quantitative absorption spectra collected from a single subject (Fitzpatrick skin type III) during both venous and arterial occlusion time courses. Blue spectra represent the baseline absorption prior to inflation of the cuff, red spectra represent the absorption during the occlusion, and green spectra represent the post-cuff-release absorption. In the case of venous occlusion, a gradual increase in absorption is observed during the occlusion phase. This trend is correlated with the expected blood pooling in the extremity (venous blood flow is stopped, yet arteries continue to pump blood into the arm). This increase is most obvious in the 530 to 580 nm region of the spectra, where there are distinct absorption features specific to hemoglobin.[35] Upon cuff release, these absorption spectra return to baseline values, consistent with expected physiological behavior.[36]

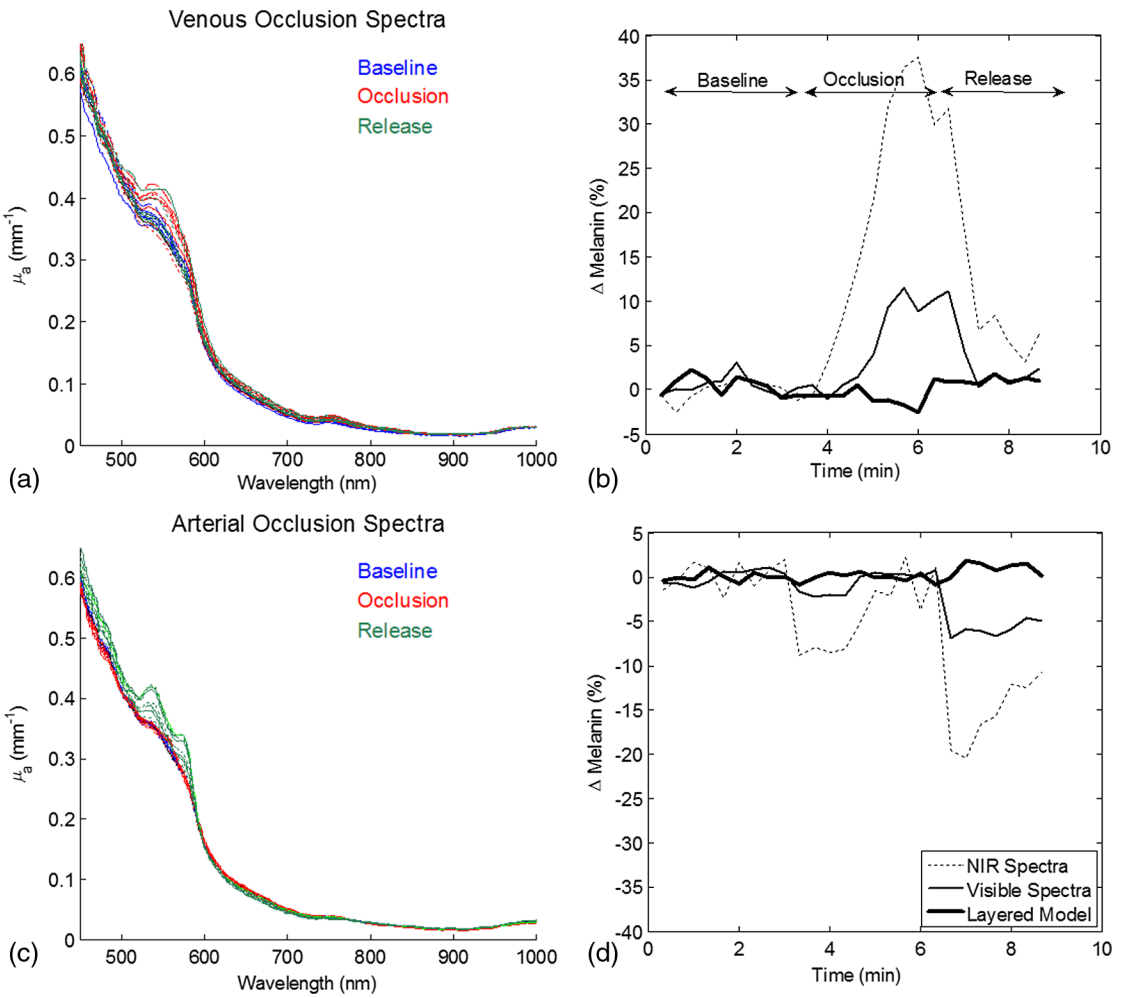

Fig. 2 Data from one subject (skin type II/III, plotted at type 2.5). (a) Measured absorption spectra from venous occlusion (90 mmHg), (b) relative, model-based change in melanin concentration determination as a function of time, during venous occlusion experiment, (c) measured absorption spectral from arterial occlusion (200 mmHg), (d) relative, model-based change in melanin concentration determination as a function of time, during arterial occlusion.

In the case of arterial occlusion, total hemoglobin concentration remains constant, as both venous and arterial blood flow is stopped. This is evidenced in the measured spectra, as there is no significant increase in overall absorption during the occlusion phase. Rather, there is an expected, gradual depletion of oxygen from blood. This is most obviously observed in the 530 to 580 nm region where the double absorption band of oxygenated hemoglobin transitions to the single band, characteristic of deoxygenated hemoglobin. Upon release, arterial occlusions are typically characterized by a hyperemic response: a large bolus of oxyhemoglobin to accommodate the high demand for oxygen in tissue that was depleted during the occlusion period.[37] This is evidenced in the measured spectra by the dramatic, dual absorption feature in the 530 to 580 nm region, associated with oxyhemoglobin.

Figures 2(b) and 2(d) present the relative change in determined melanin concentration by the three methods described in the previous section [i.e., using only NIR data (650 to 1000 nm), visible wavelength data (450 to 600 nm), and our layered model approach (450 to 1000 nm)]. In the venous occlusion case [Fig. 2(b)], both NIR and visible regime data produced increases in melanin concentration that mimicked trends produced by increases in total hemoglobin. However, when the layered model is applied, the melanin concentration estimation is held to within 2% of baseline. In the arterial occlusion case, there was a negative deviation in melanin concentration estimation using NIR spectra during the occlusion period. There were also negative deviations in melanin for both NIR and visible spectra upon cuff release that followed similar trends to the hyperemic response in blood. The layered model showed only minimal fluctuation in its estimate of melanin throughout all time periods of this occlusion experiment.

3.1 *Baseline Melanin Concentrations Reported by Each Spectral Decomposition Method*

As Fig. 3 shows, there are highly disparate values reported for melanin concentration when differing spectral regions/models are employed. This is largely due to the fact that light will interrogate tissues not just containing melanin but also tissues that underlie it. As a result, absorption signatures from melanin will only occupy a fraction of the total spectral signature detected from tissue (i.e., partial volume). Diffusely reflected light in the visible may penetrate hundreds of microns, whereas NIR may reach several millimeters, when planar illumination methods are employed.[28] The melanin concentration values determined by the layered model method, however, are consistent with volar arm mesurements reported across skin types in our previous validation study.[27]

From Fig. 3, it is also evident that the range of reported melanin values are also different, i.e., the differentiation in melanin values are not merely a scale factor. Increases in melanin concentration will additionally reduce the effective penetration depth, thereby increasing the relative contribution from superficial tissues (e.g., melanin) toward the total spectral signal measured.

Although the primary aims of this particular investigation were to compare the performance of three methods for interpreting spectral data, the layer model is unique in that it can also determine melanin layer thickness. This study measured the spectral response from the volar forearm and the layered model determined that the melanin layer thickness was 96 ± 3 μm, averaged across all subjects. This was in agreement with

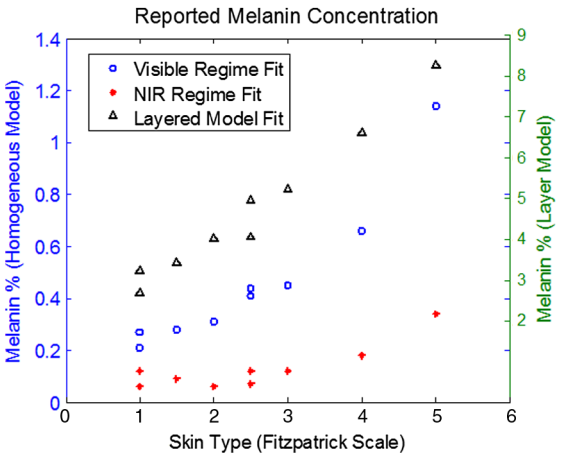

Fig. 3 Total melanin concentration (from baseline) determined by each respective spectral decomposition method. Note that as the magnitudes of the reported values scale differently between homogeneous and layered methods, visible and NIR data are scaled to the left *y*-axis, whereas the layer model data are scaled to the right *y*-axis.

previous studies[27] as expectations for epidermal thickness would reside between values from volar upper arm and dorsal forarm (locations measured in previous study and correlated to multiphoton microscopy). Additionally, these thickness values did not exhibit any correlation with phototype. As discussed in that publication, it is important to note that these thickness values are reported in terms of optical pathlength and not physical thickness.

3.2 *ΔMelanin Results*

Figures 4(a) and 4(b) show the relative percent changes from baseline melanin concentration for NIR only, Vis only, and our layered model approach across all skin types imaged in this study. The magnitude of errors are larger in the venous occlusion case, given the greater change (increase) in the overall tissue absorption due to the blood pooling that occurs during the occlusion phase of the measurements. Averaging across all skin types, there was $8.1 \pm 6.5\%$ cross-talk error derived from using NIR spectra only, $4.4 \pm 1.4\%$ from visible spectra, whereas the layered model produced mean errors of $1.4 \pm 0.8\%$. As total hemoglobin concentration is kept approximately constant during the arterial occlusion phase, total absorption values did not change significantly. There was a transition from spectral features of oxygenated to deoxygenated hemoglobin. In these arterial occlusions, the overall magnitudes of cross-talk errors were lower; however, the mean errors from the NIR regime decomposition remained relatively higher than the other methods, while the layer model approach provided the minimal error. Here, the mean cross-talk errors were $4.0 \pm 2.4\%$, $2.0 \pm 1.5\%$, and $0.6 \pm 0.3\%$ for the NIR regime, visible regime, and layered model, respectively.

3.3 *Tissue Oxygenation Results*

Figure 5 shows the baseline tissue oxygen saturation percentages (StO_2) as determined using NIR only, Vis only, and our layered model approach across all skin types imaged in this study. When only the NIR wavelength range is used to

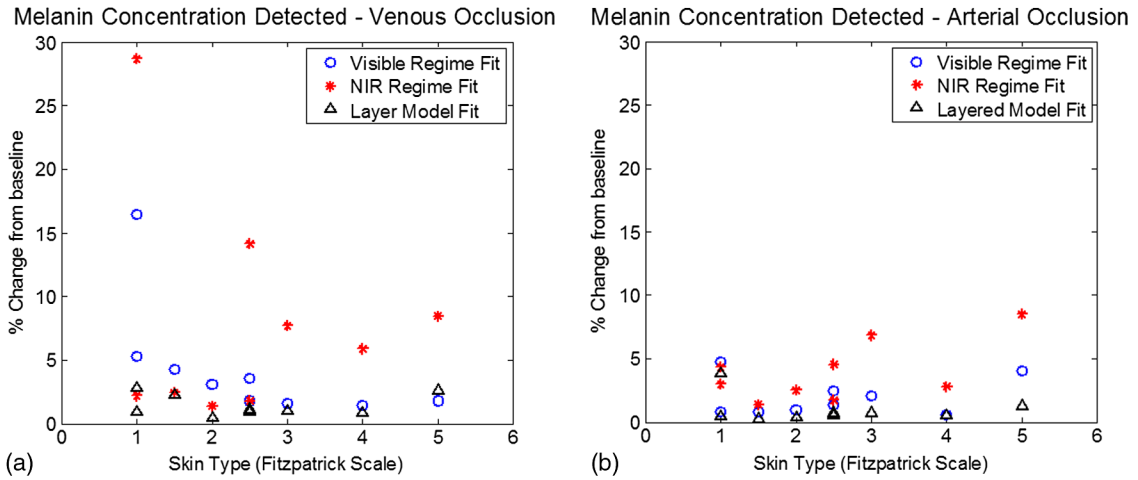

Fig. 4 ΔMelanin metric shown for each individual subject as a function of their assessed Fitzpatrick skin type. (*) depict values determined through homogeneous model fits in the NIR, (o) visible, and (Δ) depict those resulting from the layered model method.

determine StO_2, not only is there a large variance between specific subjects observed but also there is an apparent correlation between tissue oxygenation and skin type. Here, NIR determined StO_2 declines as skin pigmentation increases. When only a visible spectral range is considered, StO_2 does not appear to vary significantly as a function of skin type (pigmentation); however, these values are tightly bound between 50% and 60%, which is lower than expected from the literature.[38–40] The layered model results also appear independent from skin type; however, these values are bounded within the range of 80% to 90%, which is slightly higher than previously published, optically derived values reported in the literature. The interpretation of these results will be discussed in the following section.

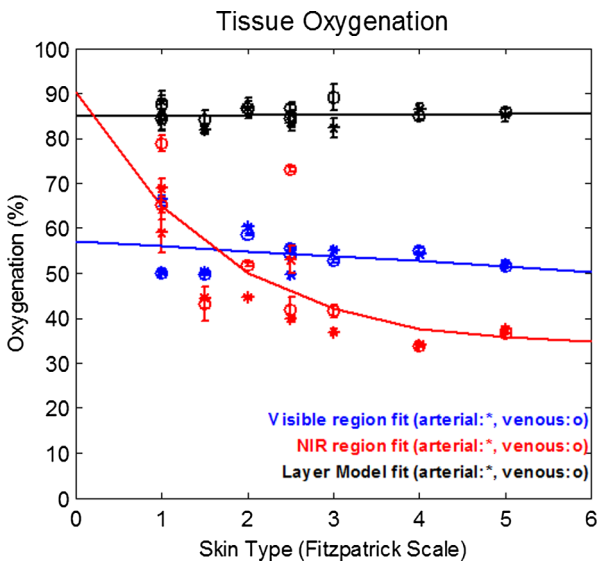

Fig. 5 Baseline tissue oxygenation (StO_2) from both venous (o) and arterial (*) occlusion measurements. Error bars represent the standard deviation of StO_2 from every time point acquired during baseline. Each measurement for venous occlusions for each subject was not acquired from the same precise tissue location as for the arterial occlusion for the same subject.

4 Discussion

The goal of this investigation is to evaluate sources of error and cross-talk based on the interpretation of "quantitative" spectral data collected from a single instrument/measurement geometry. Venous and arterial cuff occlusions were used in these experiments as they will induce a perturbation in the hemodynamics that can be temporally controlled and the generalized hemodynamic effects of these two types of occlusions are well understood, i.e., venous occlusions will induce blood pooling (increase total hemoglobin concentration) and arterial occlusions will result in a deoxygenation of hemoglobin followed by a hyperemic response upon cuff release. Whereas the magnitude of these changes is not controlled and is often subject specific, the central hypothesis of the particular study is based on the assertion that both the melanin concentration and spatial distribution remain invariant to these hemodynamic changes, irrespective of the individual magnitudes of these hemodynamic changes.

Based on this, we have developed an initial metric to evaluate whether a choice of spectral regime or layer model would be most effective in minimizing variance in the determination of melanin when deliberate hemodynamic events are produced. The ΔMelanin metric is a descriptor of how homogeneous fitting routines will induce errors (cross-talk) between depth-distributed chromophores in tissue.

In order to account for subject-specific variance, we can look at the relative improvement (i.e., reduction in ΔMelanin) on an individual subject basis. As each analysis method uses data collected at the same time points from the same measurement geometry (instrument configuration), differences between these analyses methods for any individual subject or measurement sequence will only be derived from the method alone. In this case, the layered method consistently produced lower ΔMelanin values on a subject by subject basis than those calculated when using only the NIR portion of the spectrum. This includes the ΔMelanin results under both venous and arterial occlusion conditions ($n = 18$). The layered method also outperformed the visible regime ΔMelanin results during venous and arterial occlusions with only one exception. This one case occurred with the darkest skin pigmentation subject under the venous occlusion condition. This case represented the most

extreme amount of absorption measured in the study due to the combination of highest degree of skin pigmentation along which the greatest increases of hemoglobin concentration. Even in this case, the layered model value for ΔMelanin remained within 1% of that calculated using just the visible spectrum alone.

ΔMelanin illustrates the magnitude of cross-talk error between melanin and hemoglobin; however, it remains unclear from this metric alone as to whether these errors, which were all <10%, would provide any significant impact on the calculation of actual physiologic parameters. To that end, we also examined the estimation of tissue oxygenation, StO_2, at baseline as a means to assess whether these errors in chromophore calculation would present source of concern when attempting to characterize tissue physiology through spectroscopic methods.

NIR regime-derived estimations of StO_2 values exhibit a negative correlation with skin type (pigmentation). As shown in Fig. 4, baseline StO_2 values will decrease when the amount of pigmentation (melanin) increases. This trend is contrary to expected physiology, as there is no correlation between oxygenation and degree of pigmentation. This is an indication that the NIR regime is particularly sensitive to depth dependence, spectral cross-talk artifacts between the decomposition. Given that the spectral features of hemoglobin species as well as melanin in this spectral region are both relatively weak and featureless, it is not surprising that decomposition methods may find it difficult to completely isolate these chromophores from each other. The total volume of interrogation will also change as a function of wavelength in this spectral regime. Given the depth-distributed nature of these chromophores, the resulting measured absorption spectrum is not simply a linear superposition of basis spectra; rather, it also encodes its relative, wavelength-dependent partial volume contribution toward the total signal detected. This demonstrates that, in this case, superficial pigmentation can affect measurement of tissue oxygenation, as determined by diffuse reflectance-based optical methods.

Using visible wavelengths alone, there was significantly less variation in the determined melanin concentration than was observed in the NIR regime. Given that hemoglobin absorption spectra exhibit more distinct features in the visible than in the NIR, the ability to separate these features from the relatively featureless melanin spectrum is far more robust. The amount of cross-talk present in the least-squares decomposition is significantly reduced. Similarly, the variation in interrogation depth in the visible regime is also lower than is observed in the NIR, indicating that there is little volume-based distortion of the detected spectral features in this regime. Visible light, however, is significantly limited in the depth into which it can interrogate tissue. So while it might be more robust in isolating the optical effects of hemodynamics from that of melanin, it will typically only interrogate the most superficial volumes of the dermis.

Unlike homogeneous model-based spectral decomposition methods used in this study, the layered model approach presents an opportunity to directly address the concerns identified in both visible and NIR spectroscopy. This layer model addresses difficulties associated with superficial pigmentation by segmenting tissue in depth based on the distinct spectral properties specific to layered structures in skin. Not only does this tissue segmentation account for the partial volume effects from melanin, but also this method also accounts for the spectral distortion, realizing that the contribution of melanin absorption at every wavelength will change as a function of the total volume of tissue interrogated and not just as a function of its absorption coefficient at that wavelength. As a result of these features, the layered method is able to provide a distribution of StO_2 values that have no apparent correlation with skin pigmentation.

It is worth noting, however, that these StO_2 values are higher than those derived from visible spectra alone. As noted in the discussion of the visible regime StO_2 results, the depth of penetration of detected light in the visible spectral region is significantly limited (100 μm) due to the relatively high absorption and scattering values in this window. In contrast, the layered model approach utilizes spectral information from both visible and NIR regimes. Hence, when this method determines hemoglobin concentrations, it is derived over tissue volumes several millimeters deep. The respective volume differences probed by these two methods may provide some justification as to why StO_2 values appear so disparate (50% to 60% versus 80% to 90%). It has been suggested that oxygenation within dermal tissue may not be a singular value, but rather a gradient as a function of depth.[41,42] Superficial dermal tissue may exhibit a significantly lower StO_2 relative to values found within deeper dermal tissue.

Other groups have developed three-layered models of skin as a direct result.[43–45] Spectral reflectance from skin is interpreted as contributions from the epidermal layer (melanin), as well as upper and lower dermal layers, each of which contain differing concentration of hemoglobin species. The resulting calculations of StO_2 values from this study support the results presented by these other groups.

The layered model employed in our study presents a significant opportunity to provide noninvasive, quantitative optical measurements of tissue hemodynamics, independent of an individual's skin pigmentation. The distinct advantage of this particular measurement paradigm and layered model interpretation is that it provides a quantitative measure of melanin concentration and thickness,[27] which is necessary to decouple the optical effects of melanin from that of underlying tissue chromophores. From the SFDS spectroscopic platform, we have the additional opportunity to not just interpret deep dermal tissue oxygenation and hemodynamics but also use the layer model segmentation in order to correct the visible regime data for the partial volume imparted by superficial melanin (thereby reducing the slight pigmentation dependence of visible regime calculation of hemodynamics and oxygenation).

However, for these concepts to advance and become rigorously validated, we must also acknowledge the assumptions and limitations of this current layered model. In its present form, this model assumes that the scattering of tissue is homogeneous in depth. In the model employed here, it is only distinct chromophore absorption features that differentiate layered structures. This model, as used here, also assumes that melanin can be described by a single, invariant absorption spectrum.[27]

5 Conclusion

Developing optical methods that directly address both the spectral and structural aspects of tissue are critical toward advancing imaging tools for all skin types. There are distinct advantages and significant improvement in isolating melanin from underlying hemodynamics when using a layered model approach over classic homogeneous model interpretation of skin spectra. In this study, we demonstrate that utilizing a simple, semiempirical layered model approach minimizes cross-talk between melanin

and hemoglobin concentration, outperforming methods that utilize visible or NIR spectra alone.

Acknowledgments

We thankfully recognize support from the Beckman Foundation and the NIH, including P41EB015890 (A Biomedical Technology Resource) from NIBIB and R42GM077713 from NIGMS. The content is solely the responsibility of the authors and does not necessarily represent the official views of the NIBIB or NIH.

References

1. T. D. O'sullivan et al., "Diffuse optical imaging using spatially and temporally modulated light," *J. Biomed. Opt.* **17**(7), 071311 (2012).
2. S. L. Jacques, "Optical properties of biological tissues: a review," *Phys. Med. Biol.* **58**(11), R37–R61 (2013).
3. W. F. Cheong, S. A. Prahl, and A. J. Welch, "A review of the optical-properties of biological tissues," *IEEE J. Quantum Electron.* **26**(12), 2166–2185 (1990).
4. M. G. Nichols, E. L. Hull, and T. H. Foster, "Design and testing of a white-light, steady-state diffuse reflectance spectrometer for determination of optical properties of highly scattering systems," *Appl. Opt.* **36**(1), 93–104 (1997).
5. S. H. Tseng, A. Grant, and A. J. Durkin, "In vivo determination of skin near-infrared optical properties using diffuse optical spectroscopy," *J. Biomed. Opt.* **13**(1), 014016 (2008).
6. V. T. C. Chang et al., "Quantitative physiology of the precancerous cervix in vivo through optical spectroscopy," *Neoplasia* **11**(4), 325–332 (2009).
7. F. Bevilacqua et al., "Broadband absorption spectroscopy in turbid media by combined frequency-domain and steady-state methods," *Appl. Opt.* **39**(34), 6498–6507 (2000).
8. D. J. Cuccia et al., "Quantitation and mapping of tissue optical properties using modulated imaging," *J. Biomed. Opt.* **14**(2), 024012 (2009).
9. N. Dognitz et al., "Determination of the absorption and reduced scattering coefficients of human skin and bladder by spatial frequency domain reflectometry," *Proc. SPIE* **3195**, 102–109 (1998).
10. F. Vasefi et al., "Polarization-sensitive hyperspectral imaging in vivo: a multimode dermoscope for skin analysis," *Sci. Rep.* **4**, 4924 (2014).
11. A. Mazhar et al., "Spatial frequency domain imaging of port wine stain biochemical composition in response to laser therapy: a pilot study," *Lasers Surg. Med.* **44**(8), 611–621 (2012).
12. J. Q. Nguyen et al., "Spatial frequency domain imaging of burn wounds in a preclinical model of graded burn severity," *J. Biomed. Opt.* **18**(6), 066010 (2013).
13. D. J. Rohrbach et al., "Preoperative mapping of nonmelanoma skin cancer using spatial frequency domain and ultrasound imaging," *Acad. Radiol.* **21**(2), 263–270 (2014).
14. D. J. Rohrbach et al., "Characterization of nonmelanoma skin cancer for light therapy using spatial frequency domain imaging," *Biomed. Opt. Express* **6**(5), 1761–1766 (2015).
15. R. B. Saager et al., "A light emitting diode (LED) based spatial frequency domain imaging system for optimization of photodynamic therapy of nonmelanoma skin cancer: quantitative reflectance imaging," *Lasers Surg. Med.* **45**(4), 207–215 (2013).
16. A. Yafi et al., "Postoperative quantitative assessment of reconstructive tissue status in a cutaneous flap model using spatial frequency domain imaging," *Plast. Reconstr. Surg.* **127**(1), 117–130 (2011).
17. A. Ponticorvo et al., "Quantitative assessment of graded burn wounds in a porcine model using spatial frequency domain imaging (SFDI) and laser speckle imaging (LSI)," *Biomed. Opt. Express* **5**(10), 3467–3481 (2014).
18. S. Gioux et al., "First-in-human pilot study of a spatial frequency domain oxygenation imaging system," *J. Biomed. Opt.* **16**(8), 086015 (2011).
19. A. M. Laughney et al., "System analysis of spatial frequency domain imaging for quantitative mapping of surgically resected breast tissues," *J. Biomed. Opt.* **18**(3), 036012 (2013).
20. T. T. Nguyen et al., "Novel application of a spatial frequency domain imaging system to determine signature spectral differences between infected and noninfected burn wounds," *J. Burn Care Res.* **34**(1), 44–50 (2013).
21. K. P. Nadeau et al., "Quantitative assessment of renal arterial occlusion in a porcine model using spatial frequency domain imaging," *Opt. Lett.* **38**(18), 3566–3569 (2013).
22. R. B. Saager, D. J. Cuccia, and A. J. Durkin, "Determination of optical properties of turbid media spanning visible and near-infrared regimes via spatially modulated quantitative spectroscopy," *J. Biomed. Opt.* **15**(1), 017012 (2010).
23. S. L. Jacques and D. J. McAuliffe, "The melanosome: threshold temperature for explosive vaporization and internal absorption coefficient during pulsed laser irradiation," *Photochem. Photobiol.* **53**(6), 769–775 (1991).
24. K. Terstappen et al., "Poor correlation between spectrophotometric intracutaneous analysis and histopathology in melanoma and nonmelanoma lesions," *J. Biomed. Opt.* **18**(6), 061223 (2013).
25. S. Vyas, A. Banerjee, and P. Burlina, "Estimating physiological skin parameters from hyperspectral signatures," *J. Biomed. Opt.* **18**(5), 057008 (2013).
26. D. Yudovsky and L. Pilon, "Retrieving skin properties from in vivo spectral reflectance measurements," *J. Biophotonics* **4**(5), 305–314 (2011).
27. R. B. Saager et al., "In vivo measurements of cutaneous melanin across spatial scales: using multiphoton microscopy and spatial frequency domain spectroscopy," *J. Biomed. Opt.* **20**(6), 066005 (2015).
28. R. B. Saager et al., "Method for depth-resolved quantitation of optical properties in layered media using spatially modulated quantitative spectroscopy," *J. Biomed. Opt.* **16**(7), 077002 (2011).
29. S. L. Jacques and S. A. Prahl, "Modeling optical and thermal distributions in tissue during laser irradiation," *Lasers Surg. Med.* **6**(6), 494–503 (1987).
30. F. Morales et al., "How to assess post-occlusive reactive hyperaemia by means of laser Doppler perfusion monitoring: application of a standardised protocol to patients with peripheral arterial obstructive disease," *Microvasc. Res.* **69**(1–2), 17–23 (2005).
31. T. B. Fitzpatrick, "The validity and practicality of sun-reactive skin types I through VI," *Arch. Dermatol.* **124**(6), 869–871 (1988).
32. F. Ayers et al., "Fabrication and characterization of silicone-based tissue phantoms with tunable optical properties in the visible and near infrared domain," *Proc. SPIE* **6870**, 687007 (2008).
33. R. B. Saager et al., "Multi-layer silicone phantoms for the evaluation of quantitative optical techniques in skin imaging," *Proc. SPIE* **7567**, 756706 (2010).
34. R. B. Saager et al., "Development of spatial frequency domain instrument for the quantification of layer specific optical properties of pigmented lesions," in *Biomedical Optics and 3-D Imaging*, Optical Society of America, Miami, Florida (2012).
35. W. G. Zijlstra, A. Buursma, and W. P. Meeuwsenvanderroest, "Absorption-spectra of human fetal and adult oxyhemoglobin, de-oxyhemoglobin, carboxyhemoglobin, and methemoglobin," *Clin. Chem.* **37**(9), 1633–1638 (1991).
36. M. C. Conrad, A. B. Denison, and H. D. Green, "Evaluation of venous occlusion plethysmography," *Fed. Proc.* **19**(1), 93–93 (1960).
37. K. Myers, "Investigation of peripheral arterial disease by strain gauge plethysmography," *Angiology* **15**(7), 293–304 (1964).
38. D. J. Newton et al., "Comparison of macro-lightguide and micro-lightguide spectrophotometric measurements of microvascular hemoglobin oxygenation in the tuberculin reaction in normal human skin," *Physiol. Meas.* **15**(2), 115–128 (1994).
39. M. Kobayashi et al., "Analysis of nonlinear relation for skin hemoglobin imaging," *Opt. Express* **9**(13), 802–812 (2001).
40. A. A. Stratonnikov and V. B. Loschenov, "Evaluation of blood oxygen saturation in vivo from diffuse reflectance spectra," *J. Biomed. Opt.* **6**(4), 457–467 (2001).
41. I. M. Braverman, "The cutaneous microcirculation: ultrastructure and microanatomical organization," *Microcirculation* **4**(3), 329–340 (1997).
42. M. Stucker et al., "The cutaneous uptake of atmospheric oxygen contributes significantly to the oxygen supply of human dermis and epidermis," *J. Physiol.* **538**(3), 985–994 (2002).

43. I. Fredriksson, M. Larsson, and T. Stromberg, "Inverse Monte Carlo method in a multilayered tissue model for diffuse reflectance spectroscopy," *J. Biomed. Opt.* **17**(4), 047004 (2012).
44. L. L. Randeberg et al., "In vivo spectroscopy of jaundiced newborn skin reveals more than a bilirubin index," *Acta Paediatrica* **94**(1), 65–71 (2005).
45. L. L. Randeberg, E. L. Larsen, and L. O. Svaasand, "Characterization of vascular structures and skin bruises using hyperspectral imaging, image analysis and diffusion theory," *J. Biophotonics* **3**(1–2), 53–65 (2010).

Rolf B. Saager is currently a project scientist specializing in biomedical imaging and spectroscopy at the Beckman Laser Institute, University of California (UC), Irvine. He received his PhD in optics at the University of Rochester.

Ata Sharif is currently an assistant project scientist at the Beckman Laser Institute, UC, Irvine. He received his MD from Iran, and his MBA from UC, Irvine.

Kristen M. Kelly is a professor of dermatology and surgery at the UC, Irvine. She graduated from the UC, Los Angeles Medical School and completed her Dermatology Residency at UC Irvine and a fellowship in photomedicine at the Beckman Laser Institute.

Anthony J. Durkin is currently an associate professor in the Departments of Biomedical Engineering and Surgery at the University of California, Irvine, with a primary appointment in the Beckman Laser Institute. He received his PhD in biomedical engineering from the University of Texas at Austin.